AIMS Mathematics, 10(9): 20025–20049.
DOI: 10.3934/math.2025895
Received: 25 May 2025
Revised: 06 August 2025
Accepted: 20 August 2025
Published: 01 September 2025

http://www.aimspress.com/journal/Math

Research article

Modeling rotavirus transmission with booster vaccination using fractal-fractional derivatives

Rabeb Sidaoui[1], Ashraf A. Qurtam[2], Arshad Ali[3], Muntasir Suhail[4,*], Khaled Aldwoah[5], Abdelaziz Elsayed[6,*] and E. I. Hassan[7]

[1] Department of Mathematics, College of Science, University of Ha'il, Ha'il 55473, Saudi Arabia
[2] Biology Department, College of Science, Imam Mohammad Ibn Saud Islamic University (IMSIU), Riyadh, 11432, Saudi Arabia
[3] Department of Mathematics, University of Malakand, Chakdara Dir(L), 18800, Khyber Pakhtunkhwa, Pakistan
[4] Department of Mathematics, College of Science, Qassim University, Buraydah 51452, Saudi Arabia
[5] Department of Mathematics, Faculty of Science, Islamic University of Madinah, Madinah 42351, Saudi Arabia
[6] Biology Department, Faculty of Science, Islamic University of Madinah, Madinah, Saudi Arabia
[7] Department of Mathematics and Statistics, Imam Mohammad Ibn Saud Islamic University (IMSIU), Riyadh 11432, Saudi Arabia

* **Correspondence:** Email: m.suhail@qu.edu.sa, aaelsayed@iu.edu.sa.

Abstract: Rotavirus remains a leading cause of gastroenteritis in children under five in low- and middle-income countries due to waning immunity and incomplete vaccine coverage. To address this, we propose a mathematical model to analyze the transmission dynamics with primary and booster vaccination strategies. The model is formulated using the fractal-fractional derivative in the Caputo-Fabrizio sense, which allows for the incorporation of memory effects and hereditary properties in disease evolution. The population is structured into five compartments, including booster-immunized individuals. We derive the disease-free and endemic equilibrium points and analyze their local stability. The basic reproduction number is computed to determine the threshold conditions for disease persistence. We establish the existence and Hyers-Ulam (H-U) stability of the model, and validate the results through numerical simulations using the Adams-Bashforth method (ABM), confirmed by comparison with Runge-Kutta 4th Order (RK-4) solution plots to assess the booster vaccination impact. The results reveal that booster immunization plays a significant role in reducing the infection burden, thereby highlighting its relevance in public health planning.

Keywords: rotavirus transmission; booster vaccination; fractal-fractional calculus; equilibrium points;

existence and stability analysis; numerical analysis
Mathematics Subject Classification: 26A33, 34A08, 34A12

1. Introduction

Rotavirus is one of the primary causes of acute gastroenteritis in infants and young children worldwide. First identified in 1972 by Bishop and colleagues, the virus is recognized by its characteristic wheel—like shape under an electron microscope. It causes severe gastrointestinal symptoms—most notably vomiting and recurrent watery diarrhea-which can lead to life-threatening dehydration, especially among children under five years of age [1, 2]. Nearly 95% of children globally are estimated to contract rotavirus by the age of three, with the most vulnerable age group being between four and 36 months [3]. Symptoms typically appear within 48 hours of exposure and can persist for up to eight days, often including fever, abdominal pain, nausea, and dehydration [4–6].

Rotavirus is primarily transmitted through the fecal-oral route via contaminated hands, surfaces, and objects; additionally, respiratory secretions may contribute to its spread [7–10]. With an incubation period of approximately two days [11–13], the disease poses a global health burden that is not significantly reduced by sanitation alone. Its incidence remains comparable in both developed and developing countries, thus emphasizing the importance of immunization. In response, the World Health Organization (WHO) recommended the inclusion of rotavirus vaccines in all national immunization programs as early as June 2009 [14].

Mathematical modeling has become an indispensable tool [15–17]. These models allow researchers to analyze the disease dynamics, forecast outbreaks, and evaluate the impact of various interventions. Modeling complex biological processes has become increasingly tractable with the advancement of computational tools. Several studies have focused on rotavirus transmission. For instance, [18] analyzed the combined effects of breastfeeding and vaccinations, while others proposed optimal control strategies, identified risk factors, and evaluated alternative treatment pathways [19, 20].

To enhance biological realism, some models have introduced vaccinated compartments. In [29], the following classical integer-order model was proposed to incorporate vaccinations:

$$\begin{cases} \dot{S}(t) = (1-\tau)\theta + pV(t) - \left[qI(t) + (\zeta + r)\right] S(t), \\ \dot{V}(t) = \tau\theta + \zeta S(t) - \left[\varsigma qI(t) + (p + r)\right] V(t), \\ \dot{I}(t) = \left[qS(t) + \varsigma qV(t) - (\lambda + \delta + r)\right] I(t), \\ \dot{R}(t) = \delta I(t) - rR(t), \\ S(0) = S_0, \quad V(0) = V_0, \quad I(0) = I_0, \quad R(0) = R_0. \end{cases} \tag{1.1}$$

The parameter definitions for this model are listed in Table 1. Building on this framework, Eiman et al. [30] extended the system using a fractional-order approach, analyzed the existence and uniqueness of the solutions, and explored its qualitative behavior on subintervals of time.

In recent years, fractional-order and fractal-fractional differential equations have gained traction in biological modeling due to their ability to capture memory and hereditary effects [21, 23, 25]. In particular, the Caputo-Fabrizio (CF) derivative has proven effective in modeling short-term memory in biological processes, thereby utilizing its non-singular exponential kernel. Recent applications include

hepatitis B treatment modeling [26] and the analysis of impulsive systems in Banach space using CF and Atangana-Baleanu derivatives [28].

Despite the global rollout of rotavirus vaccines, periodic outbreaks continue to occur, often due to waning immunity and limited coverage. A typical rotavirus outbreak lasts between 4–6 weeks [27]. These challenges are especially prevalent in low- and middle-income countries. As a response, several health authorities now recommend booster doses to prolong protection [31–34]. However, the long-term epidemiological effects of booster vaccinations remain poorly understood-particularly in the context of immune memory and time-varying transmission dynamics.

Traditional integer-order models often lack the flexibility to represent such complexities. Therefore, there is a growing need for advanced modeling approaches that incorporate both temporal memory and population heterogeneity. In this study, we propose a novel rotavirus transmission model using the fractal-fractional Caputo-Fabrizio derivative (FFCFD). This framework allows us to examine the influence of memory effects and booster vaccination strategies on disease dynamics. Our goal is to assess the long-term role of booster doses in suppressing outbreaks and to offer quantitative insights that can guide immunization policies.

The remainder of the paper is organized as follows: In Section 2, we present the mathematical formulation of the proposed model; Section 3 addresses the basic mathematical analysis, including equilibrium points, the basic reproduction number, and a stability analysis; Section 4 lays the foundation with essential definitions and preliminary findings; Section 5 explores the existence of solutions, thus providing a critical framework for the analysis; Section 6 investigates the stability of the solutions; a numerical scheme is demonstrated in Section 7, which details the computation of the numerical solutions; in Section 8, these solutions are simulated and visualized, accompanied by detailed discussion and interpretation, thus yielding critical insights into the underlying dynamics; and finally, Section 9 summarizes the major findings.

2. Model formulation

In this section, we formulate our proposed model by introducing a booster vaccination class in the model studied in [29, 30] to evaluate its long-term role in disease suppression and provide quantitative insights to optimize immunization policies. We propose the following system of differential equations (DEs) governed by the FFCF operator to model the transmission dynamics of a disease with booster vaccination:

$$\begin{cases} {}^{FFCF}D_{\mu}^{\kappa,\varrho}S(t) = (1-\tau)\theta + pV(t) - [qI(t) + (\zeta + r)]S(t), \\ {}^{FFCF}D_{\mu}^{\kappa,\Lambda}V(t) = \tau\theta + \zeta S(t) - \Big(\varsigma qI(t) + (p + r + \eta)\Big)V(t), \\ {}^{FFCF}D_{\mu}^{\kappa,\Lambda}I(t) = \Big(qS(t) + \varsigma qV(t) + \chi qB(t)\Big)I(t) - (\lambda + \delta + r)I(t), \\ {}^{FFCF}D_{\mu}^{\kappa,\Lambda}R(t) = \delta I(t) - rR(t), \\ {}^{FFCF}D_{\mu}^{\kappa,\Lambda}B(t) = \eta V(t) - \Big(\chi qI(t) + r\Big)B(t), \end{cases} \tag{2.1}$$

with the initial conditions:

$$S(0) = S_0, \quad V(0) = V_0, \quad I(0) = I_0, \quad R(0) = R_0, \quad B(0) = B_0.$$

In the proposed model, the notion ${}^{FFCF}D_{\mu}^{\kappa,\Lambda}$ denotes the FFCF differential operator. The model is briefly described below.

2.1. Model's description

In the formulated model, the total population N at any given time t is divided into five compartments: susceptible (S), infected with rotavirus (I), vaccinated (V), recovered (R), and who received booster doses, namely SVIRB. Owing to the short incubation period of rotavirus, the model assumes that individuals exposed to the virus move directly to the infectious stage with certainty, thereby omitting an explicit exposed class. Individuals recovering from infection join the R compartment at a recovery rate δ, and exit this class through natural death occurring at a rate r.

Although maternal antibodies acquired through breastfeeding may provide some degree of passive immunity against rotavirus [35], the model incorporates active immunization both at birth and among susceptible individuals. The inflow into the susceptible class is given by $(1-\tau)\theta$, while the vaccinated class receives new individuals at the rate $\tau\theta$, thus reflecting immunization at birth. In addition, susceptible individuals can be vaccinated at a rate ζS, but immunity from vaccination wanes over time at a rate p. The parameter ς, with $0 < \varsigma < 1$, captures the reduction in infection risk due to vaccination.

Disease-induced mortality is accounted for by the parameter λ, and recovery from infection occurs at a rate δ. Disease transmission follows a mass-action incidence form, represented as qSI, where q signifies the effective transmission rate per contact. Furthermore, individuals transition from the vaccinated group to the booster class at a rate ηV. This booster class experiences a reduction due to infection, which occurs at a rate χqIB, as well as through natural deaths, which is modeled by rB.

2.2. Parameter descriptions

The values of the parameters used in the model are listed in Table 1. These values were selected to observe the qualitative behavior of the system under various fractal-fractional orders. No real-world data fitting or statistical estimation was performed.

Table 1. Parameters and their description.

Parameters	Definition	Parameters values	Reference
N	Total population	1000	Assumed
θ	The rate at which new individuals enter the population	0.04109 day^{-1}	Assumed
τ	The entry rate of individuals through vaccination	0.01884 people day^{-1}	Assumed
r	Natural mortality rate	0.00003653 day^{-1}	Assumed
λ	Disease-induced death rate	0.00004466 day^{-1}	[29]
q	The transmission rate of infection	0.001599 day^{-1}	Assumed
δ	The rate of recovery from infection	0.1667 day^{-1}	Assumed
ς	Proportionate reduction in infection risk	0.01 day^{-1}	[29]
p	The rate at which vaccinated individuals lose immunity	0.002778 day^{-1}	[29]
ζ	Vaccination rate	0.01884 day^{-1}	Assumed
η	Booster vaccination rate	0.001 day^{-1}	Assumed
χ	Booster infection risk factor	0.0005 day^{-1}	Assumed

Our work distinguishes itself by (i) incorporating booster immunization as a separate compartment, and (ii) using the FFCF operator to evaluate long-term memory effects. These additions demonstrate the novelty and depth of our approach.

3. Equilibrium points and basic reproduction number

In this section, we analyze disease-free equilibrium (DFE) and compute the basic reproduction number R_0.

At the DFE, there is no infection in the population. Therefore, we set the following:

$$I_0^* = 0, \quad R_0^* = 0.$$

From the model, setting all derivatives to zero yields the following equilibrium equations:

$$\begin{aligned}(1-\tau)\theta + pV_0^* - (\zeta + r)S_0^* &= 0,\\ \tau\theta + \zeta S_0^* - (p + r + \eta)V_0^* &= 0,\\ \eta V_0^* - \chi q B_0^* I_0^* - rB_0^* &= 0.\end{aligned}$$

From the third equation, we directly get the following:

$$B_0^* = \frac{\eta}{r}V_0^*.$$

Now, solve the first two equations. From the first equation,

$$S_0^* = \frac{(1-\tau)\theta + pV_0^*}{\zeta + r}.$$

Substituting this expression for S_0^* into the second equation yields the following:

$$\tau\theta + \zeta\left(\frac{(1-\tau)\theta + pV_0^*}{\zeta + r}\right) = (p + r + \eta)V_0^*.$$

From this, we obtain the following:

$$\theta(\zeta + r\tau) + \zeta p V_0^* = (p + r + \eta)(\zeta + r)V_0^*.$$

Solve for V_0^*:

$$V_0^* = \frac{\theta(\zeta + r\tau)}{(p + r + \eta)(\zeta + r) - \zeta p}.$$

Now, substitute V_0^* into the expressions for S_0^* and B_0^*, to obtain the following:

$$S_0^* = \frac{\theta\left[(1-\tau) + \frac{p(\zeta + r\tau)}{(p+r+\eta)(\zeta+r)-\zeta p}\right]}{\zeta + r},$$

$$B_0^* = \frac{\eta\theta(\zeta + r\tau)}{r\left[(p + r + \eta)(\zeta + r) - \zeta p\right]}.$$

Hence, the DFE point is as follows:

$$E_0 = (S_0^*, V_0^*, 0, 0, B_0^*),$$

with V_0^*, S_0^*, and B_0^* as given above.

To find the endemic equilibrium $E^* = (S^*, V^*, I^*, R^*, B^*)$, we set the right-hand sides of the model system to zero as follows:

$$\begin{cases} 0 = (1-\tau)\theta + pV^* - [qI^* + (\zeta + r)]S^*, \\ 0 = \tau\theta + \zeta S^* - (\varsigma q I^* + p + r + \eta)\, V^*, \\ 0 = (qS^* + \varsigma q V^* + \chi q B^*)\, I^* - (\lambda + \delta + r) I^*, \\ 0 = \delta I^* - rR^*, \\ 0 = \eta V^* - (\chi q I^* + r) B^*. \end{cases} \tag{3.1}$$

From the 1st equation,

$$S^* = \frac{(1-\tau)\theta + pV^*}{qI^* + \zeta + r}. \tag{3.2}$$

From the 2nd equation,

$$V^* = \frac{\tau\theta + \zeta S^*}{\varsigma q I^* + p + r + \eta}. \tag{3.3}$$

From the 4th equation,

$$R^* = \frac{\delta I^*}{r}. \tag{3.4}$$

From the 5th equation,

$$B^* = \frac{\eta V^*}{\chi q I^* + r}. \tag{3.5}$$

Substitute B^* in the third equation of the system, we obtain the following:

$$qS^* + \varsigma q V^* + \chi q \left(\frac{\eta V^*}{\chi q I^* + r} \right) = \lambda + \delta + r. \tag{3.6}$$

From (3.2), substitute the expression for S^* into (3.6), we obtain the following:

$$q \left(\frac{(1-\tau)\theta + pV^*}{qI^* + \zeta + r} \right) + \varsigma q V^* + \frac{\chi q \eta V^*}{\chi q I^* + r} = \lambda + \delta + r. \tag{3.7}$$

Let us isolate V^* from the above equation:

$$\frac{q(1-\tau)\theta}{qI^* + \zeta + r} + V^* \left[\frac{qp}{qI^* + \zeta + r} + \varsigma q + \frac{\chi q \eta}{\chi q I^* + r} \right] = \lambda + \delta + r. \tag{3.8}$$

Solve for V^*:

$$V^* = \frac{\lambda + \delta + r - \dfrac{q(1-\tau)\theta}{qI^* + \zeta + r}}{\dfrac{qp}{qI^* + \zeta + r} + \varsigma q + \dfrac{\chi q \eta}{\chi q I^* + r}}. \tag{3.9}$$

Now, plug S^* from (3.2) into (3.3) as follows:

$$V^* = \frac{\tau\theta + \dfrac{\zeta((1-\tau)\theta + pV^*)}{qI^* + \zeta + r}}{\varsigma qI^* + p + r + \eta}. \tag{3.10}$$

Multiply both sides by the denominator, isolate V^*, and equate with (3.9). This yields a rational expression in I^*. After algebraic simplification, we obtain the following polynomial:

$$P(I^*) = A_3(I^*)^3 + A_2(I^*)^2 + A_1 I^* + A_0 = 0, \tag{3.11}$$

where

$$\begin{cases} A_3 = \chi q^2\left[(\zeta + r)(\lambda + \delta + r) + \varsigma\zeta q\right], \\ A_2 = q\left[(\zeta + r)(\lambda + \delta + r)(p + r + \eta) + \varsigma\zeta q(p + r + \eta) + \chi q^2\eta\theta\right], \\ A_1 = q\eta\theta\left[(\lambda + \delta + r)(1 - \tau) + \varsigma q(p + r + \eta)\right], \\ A_0 = -\eta\theta(\lambda + \delta + r)(1 - \tau)(p + r + \eta). \end{cases} \tag{3.12}$$

The endemic equilibrium exists if and only if the polynomial $P(I^*)$ has at least one positive real root. This root can be used to compute all remaining equilibrium variables: S^*, V^*, R^*, and B^*.

To confirm the existence of positive real roots of the polynomial, we use Descartes' rule of signs. We see that

$$\begin{cases} A_3 = \chi q^2\left[(\zeta + r)(\lambda + \delta + r) + \varsigma\zeta q\right] > 0, \\ A_2 = q\left[(\zeta + r)(\lambda + \delta + r)(p + r + \eta) + \varsigma\zeta q(p + r + \eta) + \chi q^2\eta\theta\right] > 0, \\ A_1 = q\eta\theta\left[(\lambda + \delta + r)(1 - \tau) + \varsigma q(p + r + \eta)\right] > 0, \\ A_0 = -\eta\theta(\lambda + \delta + r)(1 - \tau)(p + r + \eta) < 0. \end{cases} \tag{3.13}$$

Thus, there is one sign change. Hence, by Descartes' rule of signs [36], the polynomial $P(I^*)$ has exactly one positive real root. Therefore, the system has a unique endemic equilibrium point.

Basic Reproduction Number: R_0 :

We use the next generation matrix method to derive R_0. From the third equation, we have the following:

$$\frac{dI}{dt} = \Big(qS + \varsigma qV + \chi qB - (\lambda + \delta + r)\Big)I.$$

From this equation, we can define the new infection vector as

$$\mathscr{F} = [qSI + \chi qBI + \varsigma qVI],$$

and the transition terms as

$$\mathscr{V} = (\lambda + \delta + r)I.$$

At the DFE, $I = 0$, and we use S_0^*, V_0^* as DFE values.

Using $R_0 = \frac{\mathscr{F}}{\mathscr{V}}$, we have the following:

$$R_0 = \frac{q}{\lambda + \delta + r}\left(\frac{(1-\tau)\theta + pV_0^*}{\zeta + r} + \left[\varsigma + \chi \cdot \frac{\eta}{r}\right]V_0^*\right), \tag{3.14}$$

where

$$V_0^* = \frac{\theta(\zeta + r\tau)}{(p + r + \eta)(\zeta + r) - \zeta p}.$$

The expression for R_0 determines whether the infection will spread in the population or die out. If $R_0 < 1$, the DFE point will be asymptotically stable; if $R_0 > 1$, it will be unstable, and the disease will spread within the population.

In the following figure, we demonstrate the sensitivity analysis of the basic reproduction number R_0 with respect to the booster vaccination rate η.

In Figure 1, we see that as η increases, the value of R_0 monotonically decreases. This indicates that a higher booster coverage contributes to a lower transmission potential of the disease. The plot clearly illustrates that booster vaccination is an effective intervention. By maintaining a moderate-to-high value of η, the infection can be significantly suppressed or even eliminated.

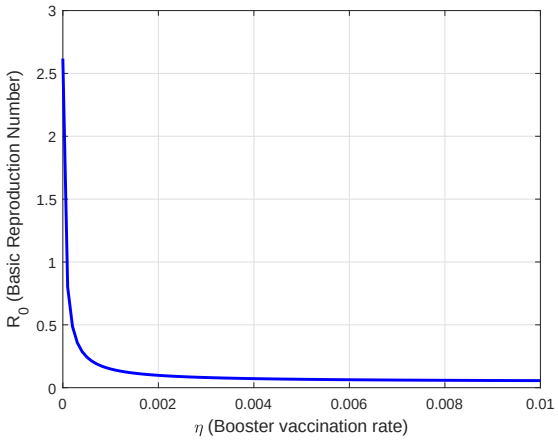

Figure 1. Effect of booster vaccination rate η on R_0.

In Figure 2, we demonstrate the sensitivity analysis of the basic reproduction number R_0 with respect to the booster transmission risk factor χ.

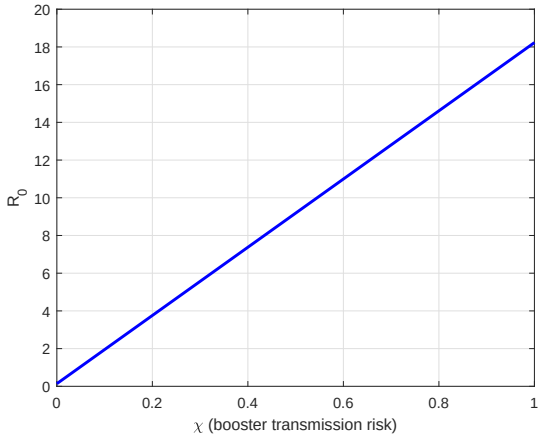

Figure 2. Effect of booster transmission risk factor χ on R_0.

From Figure 2, we observe that the booster transmission risk factor χ has a significant impact on R_0. A higher χ implies a lower efficacy of booster immunization in reducing transmission. Similarly, when $\chi = 0$, the booster class does not contribute to transmission. As $\chi \to 1$, the contribution of the booster class to transmission significantly increases, thus raising R_0. For large values of χ, the booster shots may fail to prevent infection, possibly due to waning immunity or a poorly matched vaccine strain.

To discuss the stability at equilibrium points, we compute the Jacobian matrix as follows.

$$J = \begin{bmatrix} \frac{\partial f_1}{\partial S} & \frac{\partial f_1}{\partial V} & \frac{\partial f_1}{\partial I} & \frac{\partial f_1}{\partial R} & \frac{\partial f_1}{\partial B} \\ \frac{\partial f_2}{\partial S} & \frac{\partial f_2}{\partial V} & \frac{\partial f_2}{\partial I} & \frac{\partial f_2}{\partial R} & \frac{\partial f_2}{\partial B} \\ \frac{\partial f_3}{\partial S} & \frac{\partial f_3}{\partial V} & \frac{\partial f_3}{\partial I} & \frac{\partial f_3}{\partial R} & \frac{\partial f_3}{\partial B} \\ \frac{\partial f_4}{\partial S} & \frac{\partial f_4}{\partial V} & \frac{\partial f_4}{\partial I} & \frac{\partial f_4}{\partial R} & \frac{\partial f_4}{\partial B} \\ \frac{\partial f_5}{\partial S} & \frac{\partial f_5}{\partial V} & \frac{\partial f_5}{\partial I} & \frac{\partial f_5}{\partial R} & \frac{\partial f_5}{\partial B} \end{bmatrix}. \tag{3.15}$$

Compute the partial derivatives as follows:

$$J = \begin{bmatrix} -r - \zeta - Iq & p & -Sq & 0 & 0 \\ \zeta & -\eta - r - p - Iq\varsigma & -Vq\varsigma & 0 & 0 \\ Iq & Iq\varsigma & Sq - \delta - \lambda - r + B\chi q + Vq\varsigma & 0 & I\chi q \\ 0 & 0 & \delta & -r & 0 \\ 0 & \eta & B\chi q & 0 & -r - I\chi q \end{bmatrix}. \tag{3.16}$$

At the DFE point E_0, the Jacobian matrix is given by the following:

$$J(E_0) = \begin{bmatrix} -(r+\zeta) & p & -qS_0 & 0 & 0 \\ \zeta & -(\eta + r + p) & -\varsigma qV_0 & 0 & 0 \\ 0 & 0 & (qS_0 + \varsigma qV_0 + \chi qB_0) - (\lambda + \delta + r) & 0 & 0 \\ 0 & 0 & \delta & -r & 0 \\ 0 & \eta & \chi qB_0 & 0 & -r \end{bmatrix}.$$

The third eigenvalue, associated with the infected class I, is as follows:

$$\lambda_3 = (qS_0 + \varsigma qV_0 + \chi qB_0) - (\lambda + \delta + r).$$

We may write the equation as follows:

$$\lambda_3 = \frac{(qS_0 + \varsigma qV_0 + \chi qB_0)(\lambda + \delta + r)}{(\lambda + \delta + r)} - (\lambda + \delta + r) = (\lambda + \delta + r)(R_0 - 1),$$

which is negative if and only if $R_0 < 1$.

To analyze the remaining four eigenvalues, we consider the following two submatrices.

The top-left 2×2 submatrix for the (S, V) subsystem is as follows:

$$A = \begin{bmatrix} -(r+\zeta) & p \\ \zeta & -(\eta + r + p) \end{bmatrix}.$$

The trace and determinant of A are

$$\mathrm{Tr}(A) = -(2r + \zeta + \eta + p) < 0, \quad \det(A) = (r+\zeta)(\eta + r + p) - p\zeta > 0, \textit{respectively}.$$

Therefore, both eigenvalues of A have negative real parts.

The bottom-right 2×2 submatrix for the (R, B) subsystem is as follows:

$$D = \begin{bmatrix} -r & 0 \\ \eta & -r \end{bmatrix}.$$

This is a lower triangular matrix with both diagonal entries equal to $-r < 0$. Hence, both eigenvalues of D are $-r$.

As a result, all eigenvalues of the Jacobian matrix at the DFE point are negative when $R_0 < 1$, which implies that E_0 is locally asymptotically stable under this condition.

4. Materials and methods

In the following section, we present the necessary theoretical background and analytical tools. These include definitions from fractal-fractional calculus that involve FFCFDs and fractal-fractional Riemann-Liouville (FFRL) integrals with various kernels.

Definition 4.1. [21] Let $\Omega(\mu)$ be a continuous function and fractally differentiable on the interval (a, b) of order Λ. Then, its FFCFD derivative of order κ with an exponential decay kernel is given by the following:

$$^{FFCF}D^{\kappa,\Lambda}\Omega(\mu) = \frac{M(\kappa)}{1-\kappa}\int_0^{\mu} \frac{d}{dy^{\Lambda}}\Omega(y)\exp\left(-\frac{\kappa}{1-\kappa}(\mu - y)\right)dy, \quad \mu \in [0, T], \tag{4.1}$$

where $0 < \kappa, \Lambda \leq 1$, and $M(\kappa)$ is a normalization function such that $M(0) = M(1) = 1$.

Definition 4.2. [21] Let $\Omega(\mu)$ be a continuous function and fractally differentiable on the interval (a, b) of order Λ. Then, its FFCFD of order κ is defined using a power-law kernel as follows:

$$^{FFCF}D^{\kappa,\Lambda}\Omega(\mu) = \frac{1}{\Gamma(1-\kappa)}\int_0^{\mu} \frac{d}{dy^{\Lambda}}\Omega(y)(\mu - y)^{-\kappa}dy, \quad \mu \in [0, T], \tag{4.2}$$

where $0 < \kappa, \Lambda \leq 1$, and

$$\frac{d}{dy^{\Lambda}}\Omega(y) = \lim_{\mu \to y}\frac{\Omega(\mu) - \Omega(y)}{\mu^{\Lambda} - y^{\Lambda}}. \tag{4.3}$$

Definition 4.3. [21] Let $\Omega \in C(0, T)$; then, the FFRL integral of the function $\Omega(\mu)$ with an exponential decay kernel is given by the following:

$$^{FFRL}I^{\kappa,\Lambda}\Omega(\mu) = \frac{\Lambda(1-\kappa)\mu^{\Lambda-1}\Omega(\mu)}{M(\kappa)} + \frac{\kappa\ Lambda}{M(\kappa)}\int_a^{\mu} y^{\kappa-1}\Omega(y)dy. \tag{4.4}$$

Definition 4.4. [21] Let $\Omega \in C(0, T)$; then, the FFRL integral of the function $\Omega(\mu)$ with a power-law kernel is given as follows:

$$^{FFRL}I^{\kappa,\Lambda}\Omega(\mu) = \frac{\Lambda}{\Gamma(\kappa)}\int_a^{\mu} (\mu - y)^{\kappa-1}y^{\Lambda-1}\Omega(y)dy. \tag{4.5}$$

Theorem 4.5. *(Krasnoselskii's fixed point theorem) [22] Let* $(\mathbb{X}, \|.\|)$ *be a Banach space, and let* $\mathfrak{B}$ *be its nonempty closed convex subset. Let* $\mathbb{Q}_1$ *and* $\mathbb{Q}_2$ *be the two operators that map* $\mathfrak{B}$ *into* $\mathbb{X}$ *such that*

- $\mathbb{Q}_1 x + \mathbb{Q}_2 y$ *whenever* $x, y \in \mathfrak{B}$*;*
- $\mathbb{Q}_1$ *is a contraction mapping; and*
- $\mathbb{Q}_2$ *is a continuous and compact.*

Then, there exists $z \in \mathfrak{B}$ *such that* $z = \mathbb{Q}_1 z + \mathbb{Q}_2 z$.

Definition 4.6. [24] The Adams-Bashforth method to numerically solve ordinary differential equations can be described by the following scheme:

$$x_{\ell+1} = x_\ell + h \sum_{i=1}^{r} a_i f(t_{\ell-i}, x_{\ell-i}),$$

where x_ℓ represents the numerical approximation at time t_ℓ, h denotes the time step size, $f(x,t)$ is the given ordinary differential equation, and a_i are method-specific coefficients that depend on the order of the method.

Lemma 4.7. *The solution of*

$$\begin{aligned} {}^{FFC}D^{\kappa,\Lambda}\Omega(t) &= h(t), \quad \kappa \in (0,1], \\ \Omega(0) &= \Omega_0, \end{aligned}$$

is given by

$$\Omega(t) = \Omega_0 + \frac{\Lambda}{\Gamma(\kappa)} \int_0^t x^{\Lambda-1}(t-x)^{\kappa-1} h(x)dx, \quad t \in \Upsilon. \tag{4.6}$$

Proof. We omit the proof as it is straightforward. □

5. Existence results of the proposed model

We proceed with the fixed point theory and a functional analysis to examine the existence, uniqueness, and stability of solutions for the proposed model (2.1).

Let the interval $[0, T]$ be represented by $\mathbb{I}$; we define a suitable Banach space accordingly as follows:

$$\mathfrak{B} = C(\mathbb{I}, \mathbb{R}^+) \times C(\mathbb{I}, \mathbb{R}^+) \times C(\mathbb{I}, \mathbb{R}^+) \times C(\mathbb{I}, \mathbb{R}^+) \times C(\mathbb{I}, \mathbb{R}^+)$$

equipped with the norm

$$\|\Omega\| = \max\{|S(\mu)| + |V(\mu)| + |I(\mu)| + |R(\mu)| + |B(\mu)|\},$$

$S, V, I, R, B \in \mathfrak{B}$.

Problem (2.1) can be formulated as follows:

$$\begin{cases} {}^{FFCF}D_{\mu}^{\kappa,\Lambda}\Omega(\mu) = \Omega_1(\mu, S, V, I, R, B), \\ {}^{FFCF}D_{\mu}^{\kappa,\Lambda}\Omega(\mu) = \Omega_2(\mu, S, V, I, R, B), \\ {}^{FFCF}D_{\mu}^{\kappa,\Lambda}\Omega(\mu) = \Omega_3(\mu, S, V, I, R, B), \\ {}^{FFCF}D_{\mu}^{\kappa,\Lambda}\Omega(\mu) = \Omega_4(\mu, S, V, I, R, B), \\ {}^{FFCF}D_{\mu}^{\kappa,\Lambda}\Omega(\mu) = \Omega_5(\mu, S, V, I, R, B). \end{cases} \tag{5.1}$$

Its compact form is given by the following:

$${}^{FFCF}D_{\mu}^{\kappa,\Lambda}\Omega(\mu) = \begin{cases} g(\mu, \Omega(\mu)), \\ \Omega(0) = \Omega_0, \quad \mu \in \mathbb{I}, \end{cases} \tag{5.2}$$

where the vector $\Omega(\mu) = (S, V, I, R, B)$ denotes the variable with the specific initial condition Ω_0, and the variable function g takes the form:

$$g(\mu, \Omega(\mu)) = \begin{bmatrix} \Omega_1(\mu, S, V, I, R, B) \\ \Omega_2(\mu, S, V, I, R, B) \\ \Omega_3(\mu, S, V, I, R, B) \\ \Omega_4(\mu, S, V, I, R, B) \\ \Omega_5(\mu, S, V, I, R, B) \end{bmatrix},$$

and

$$\Omega(\mu) = \begin{bmatrix} \Omega_1 \\ \Omega_2 \\ \Omega_3 \\ \Omega_4 \\ \Omega_5 \end{bmatrix} = \begin{bmatrix} (1-\tau)\theta + pV(t) - [qI(t) + (\zeta + r)]S(t) \\ \tau\theta + \zeta S(t) - \Big(\varsigma qI(t) + (p + r + \eta)\Big)V(t) \\ \Big(qS(t) + \varsigma qV(t) + \chi qB(t)\Big)I(t) - (\lambda + \delta + r)I(t) \\ \delta I(t) - rR(t) \\ \eta V(t) - \Big(\chi qI(t) + r\Big)B(t) \end{bmatrix}, \Omega_0 = \begin{bmatrix} S_0 \\ V_0 \\ I_0 \\ R_0 \\ B_0 \end{bmatrix}.$$

Lemma 5.1. *Problem*

$${}^{FFCF}D_{\mu}^{\kappa,\Lambda}\Omega(\mu) = \begin{cases} \varphi(\mu), & 0 < \kappa, \Lambda \leq 1, \ if\, \mu \in [0, T], \\ & \Omega(0) = \Omega_0, \end{cases} \tag{5.3}$$

has the solution

$$\Omega(\mu) = \Omega_0 + \frac{\Lambda(1-\kappa)\mu^{\Lambda-1}\varphi(\mu)}{M(\kappa)} + \frac{\kappa\Lambda}{M(\kappa)}\int_0^{\mu} y^{\kappa-1}\varphi(y)dy, \quad \mu \in \mathbb{I}. \tag{5.4}$$

Corollary 1. *By Lemma 5.1, the solution to the problem* (5.2) *of the proposed model can be expressed as follows:*

$$\Omega(\mu) = \Omega_0 + \frac{\Lambda(1-\kappa)\mu^{\Lambda-1}g(\mu, \Omega(\mu))}{M(\kappa)} + \frac{\kappa\Lambda}{M(\kappa)}\int_0^{\mu} y^{\kappa-1}g(y, \Omega(y))dy, \quad \mu \in \mathbb{I}. \tag{5.5}$$

We introduce the operator $W : \mathfrak{B} \to \mathfrak{B}$ by

$$W(\Omega) = \Omega_0 + \frac{\Lambda(1-\kappa)\mu^{\Lambda-1}g(\mu,\Omega(\mu))}{M(\kappa)} + \frac{\kappa\Lambda}{M(\kappa)}\int_0^\mu y^{\kappa-1}g(y,\Omega(y))dy, \quad \mu \in \mathbb{I}. \tag{5.6}$$

To obtain the results, we need to take the following necessary assumptions:

(A_1) Let there exist some constants say $L_g > 0$ such that for $\Omega, \overline{\Omega} \in \mathfrak{B}$, we have

$$|g(\mu,\Omega(\mu)) - g(\mu,\overline{\Omega}(\mu))| \leq L_g|\Omega - \overline{\Omega}|;$$

(A_2) Assume that there exist constants C_g, and $M_g > 0$ such that

$$|g(\mu,\Omega(\mu))| \leq C_g|\Omega(\mu)| + M_g.$$

Theorem 5.2. *If assumptions* (A_1)*–*(A_2) *hold, then problem* (5.2) *has at least one solution.*

Proof. We change (5.2) into a fixed point problem by the following:

$$\Omega = W(\Omega(\mu)), \quad \Omega \in \mathfrak{B}.$$

We consider a close ball $\Theta_\theta = \{\Omega \in \mathfrak{B} : \|\Omega\| \leq \theta\}$ with

$$\theta \geq \frac{|\Omega_0| + \frac{M_g\Lambda}{M(\kappa)}\left((1-\kappa)T^{\Lambda-1} + T^\kappa\right)}{1 - \frac{C_g\Lambda}{M(\kappa)}\left((1-\kappa)T^{\Lambda-1} + T^\kappa\right)}.$$

We take the operator W as the sum of the two sub operators W_1 and W_2 such that

$$W_1\Omega(\mu) = \left\{\Omega_0 + \frac{\Lambda(1-\kappa)\mu^{\Lambda-1}g(\mu,\Omega(\mu))}{M(\kappa)}, \right. \tag{5.7}$$

and

$$W_2\Omega(\mu) = \left\{\frac{\kappa\Lambda}{M(\kappa)}\int_0^\mu y^{\kappa-1}g(y,\Omega(y))dy. \right. \tag{5.8}$$

Several steps are involved in accomplishing the proof.
Step 1: $W_1\Omega(\mu) + W_2\Omega(\mu) \in \Theta_\theta$. For $\mu \in \mathbb{I}$, $\Omega \in \Theta_\theta$, with (A_2), we have the following:

$$\begin{aligned}
|W_1\Omega(\mu) + W_2\Omega(\mu)| &= \left|\Omega(\mu_0) + \frac{\Lambda(1-\kappa)\mu^{\Lambda-1}g(\mu,\Omega(\mu))}{M(\kappa)} + \frac{\kappa\Lambda}{M(\kappa)}\int_0^\mu y^{\kappa-1}g(y,\Omega(y))dy\right| \\
&\leq |\Omega_0| + \frac{\Lambda(1-\kappa)\mu^{\Lambda-1}|g(\mu,\Omega(\mu))|}{M(\kappa)} + \frac{\kappa\Lambda}{M(\kappa)}\int_0^\mu y^{\kappa-1}|g(y,\Omega(y))|dy \\
&\leq |\Omega_0| + \frac{M_g\Lambda}{M(\kappa)}\left((1-\kappa)T^{\Lambda-1} + T^\kappa\right) + \frac{C_g\Lambda}{M(\kappa)}\left((1-\kappa)T^{\Lambda-1} + T^\kappa\right)\theta \leq \theta.
\end{aligned} \tag{5.9}$$

Hence, $W_1\Omega(\mu) + W_2\Omega(\mu) \in \Theta_\theta$.
Step 2: W_1 is a contraction.

For $\mu \in \mathbb{I}$, $\Omega_1, \Omega_2 \in \Theta_\theta$, then

$$\begin{aligned} |W_1\Omega_1(\mu) - W_1\Omega_2(\mu)| &= \max_{\mu\in[0,T]} \left(|\Omega_1(\mu_1) - \Omega_2(\mu_1)| + \frac{\Lambda(1-\kappa)\mu^{\Lambda-1}}{M(\kappa)} |g(\mu, \Omega_1(\mu)) - g(\mu, \Omega_2(\mu))| \right) \\ &\leq \left(1 + \frac{\Lambda(1-\kappa)T^{\Lambda-1}L_g}{M(\kappa)}\right) \|\Omega_1 - \Omega_2\|. \end{aligned} \tag{5.10}$$

If $1 + \frac{\Lambda(1-\kappa)T^{\Lambda-1}L_g}{M(\kappa)} \leq 1$, then W_1 is a contraction.

Step 3: In this step, we demonstrate the relative compactness of W_2. Specifically, we show that W_2 is continuous, uniformly bounded on Θ_θ, and equi-continuous.

W_2 is continuous due to the continuity of $g(\mu, \Omega(\mu))$.

W_2 is uniformly bounded on Θ_θ :

For $\mu \in \mathbb{I}$, $\Omega \in \Theta_\theta$, we consider the following:

$$\begin{aligned} |W_2\Omega(\mu)| &= \frac{\kappa\Lambda}{M(\kappa)} \int_0^\mu y^{\kappa-1} |g(y, \Omega(y))| \, dy \\ &\leq \left(C_g|\theta| + M_g\right) \frac{\Lambda}{M(\kappa)} T^\kappa \leq \theta. \end{aligned} \tag{5.11}$$

Thus, W_2 is uniformly bounded on Θ_θ.

Next, we need to establish equi-continuity.

Let $\mu_a, \mu_b \in \mathbb{I}$ with $\mu_a < \mu_b$. Then,

$$\begin{aligned} \|W_2\Omega(\mu_b) - W_2\Omega(\mu_a)\| &\leq \frac{\kappa\Lambda}{M(\kappa)} \int_0^{\mu_b} y^{\Lambda-1} |g(y, \Omega(y))| \, dy - \frac{\kappa\Lambda}{M(\kappa)} \int_0^{\mu_a} y^{\Lambda-1} |g(y, \Omega(y))| \, dy \\ &\leq \frac{\kappa\Lambda}{M(\kappa)} \left(\int_0^{\mu_b} y^{\Lambda-1} |g(y, \Omega(y))| \, dy - \int_0^{\mu_a} y^{\Lambda-1} |g(y, \Omega(y))| \, dy \right) \\ &= \frac{\kappa}{M(\kappa)} \left((\mu_b)^\Lambda - (\mu_a)^\Lambda \right) \left(C_g\theta + M_g \right) \\ &\to 0 \text{ as } \mu_b \to \mu_a. \end{aligned}$$

This proves that W_2 is equi-continuous. Thus, W is relatively compact by the Arzelá-Ascoli theorem, and its complete continuity is ensured by the aforementioned steps. By Theorem 4.5, it follows that there is at least one solution for problem (5.2). □

Theorem 5.3. *Under assumption* (A_1) *and the condition* $\frac{L_g}{M(\kappa)} \left(\Lambda (1-\kappa) T^{\Lambda-1} + \kappa T^\Lambda \right) < 1$, *the problem of model* (5.2) *has a unique solution.*

Proof. For $\mu \in \mathbb{I}$, $\Omega_1, \Omega_2 \in \Theta_\theta$, we have the following:

$$\begin{aligned} |W\Omega_1(\mu) - W\Omega_2(\mu)| &\leq \max_{\mu\in\mathbb{I}} \left[\frac{(1-\kappa)}{M(\kappa)} \Lambda\mu^{\Lambda-1} |g(\mu, \Omega_1(\mu)) - g(\mu, \Omega_2(\mu))| \right. \\ &+ \left. \frac{\kappa\Lambda}{\mathbb{M}(\kappa)} \int_0^\mu y^{\Lambda-1} |g(y, \Omega_1(y)) - g(y, \Omega_2(y))| \, dy \right] \\ &\leq \max_{\mu\in\mathbb{I}} \left[\frac{(1-\kappa)L_g}{M(\kappa)} \Lambda\mu^{\Lambda-1} |\Omega_1(\mu) - \Omega_2(\mu)| \right. \end{aligned}$$

$$+ \quad \frac{\kappa L_g T^{\Lambda}}{M(\kappa)} |\Omega_1(\mu) - \Omega_2(\mu)| \Big].$$

Hence,

$$\|W\Omega_1 - W\Omega_2\| \leq \frac{L_g}{M(\kappa)} \left(\Lambda (1-\kappa) T^{\Lambda-1} + \kappa T^{\Lambda}\right) \|\Omega_1 - \Omega_2\|.$$

Since $\frac{L_g}{M(\kappa)} \left(\Lambda (1-\kappa) T^{\Lambda-1} + \kappa T^{\Lambda}\right) < 1$, W is a contraction; thus, the solution of model (5.2) is unique. □

6. Hyers-Ulam (H-U) stability

In this section, we investigate Hyers-Ulam (HU) stability of the proposed problem. H-U stability ensures the robustness of the system's solutions under small perturbations, which is crucial in real-world epidemic modeling due to uncertainties in the data, parameters, or initial conditions. This implies that the predicted trajectories of infected or immunized individuals remain reliable even under slight variations, thus supporting the model's practical applicability in policy planning.

We adopted the following definitions from the manuscript [37].

Definition 6.1. The model prescribed by (5.2) is said to be HU stable if there is a real number $\mathbf{c} > 0$ such that for each $\epsilon > 0$, any solution $\widehat{\Omega} \in \mathfrak{B}$ of the inequality

$$\left| {}^{PFFCF}D_{\mu}^{\kappa,\Lambda}\widehat{\Omega}(\mu) - g(\mu, \widehat{\Omega}(\mu)) \right| \leq \epsilon, \quad \mu \in \mathbb{I},$$

and the unique solution $\Omega \in \mathfrak{B}$ of the model (5.2) satisfy the following inequality:

$$\left\| \widehat{\Omega} - \Omega \right\| \leq \mathbf{c}\epsilon, \qquad \mu \in \mathbb{I},$$

where

$$\widehat{\Omega}(\mu) = \begin{pmatrix} \widehat{S}(\mu) \\ \widehat{V}(\mu) \\ \widehat{I}(\mu) \\ \widehat{R}(\mu) \\ \widehat{B}(\mu) \end{pmatrix}, \widehat{\Omega}(0) = \begin{pmatrix} \widehat{S}(0) \\ \widehat{V}(0) \\ \widehat{I}(0) \\ \widehat{R}(0) \\ \widehat{B}(0) \end{pmatrix}, g(\mu, \widehat{\Omega}(\mu)) = \begin{pmatrix} \widehat{\Omega_1}(\mu, \widehat{S}, \widehat{V}, \widehat{I}, \widehat{R}, \widehat{B}) \\ \widehat{\Omega_2}(\mu, \widehat{S}, \widehat{V}, \widehat{I}, \widehat{R}, \widehat{B}) \\ \widehat{\Omega_3}(\mu, \widehat{S}, \widehat{V}, \widehat{I}, \widehat{R}, \widehat{B}) \\ \widehat{\Omega_4}(\mu, \widehat{S}, \widehat{V}, \widehat{I}, \widehat{R}, \widehat{B}) \\ \widehat{\Omega_5}(\mu, \widehat{S}, \widehat{V}, \widehat{I}, \widehat{R}, \widehat{B}) \end{pmatrix}.$$

Remark 1. Let there exist a small perturbation $\Psi \in \mathfrak{B}$ such that

(i) $|\Psi(\mu)| \leq \epsilon$, $\mu \in \mathbb{I}$; and

(ii) ${}^{PFFCF}D_{\mu}^{\kappa,\Lambda}\widehat{\Omega}(\mu) = g(\mu, \widehat{\Omega}(\mu)) + \Psi(\mu)$, $\mu \in \mathbb{I}$.

A perturbed problem solution is derived by Remark 1 as follows:

$$\begin{cases} {}^{PFFCF}D_{\mu}^{\kappa,\Lambda}\widehat{\Omega}(\mu) = g(\mu, \widehat{\Omega}(\mu)) + \Psi(\mu), \\ \widehat{\Omega}(0) = \widehat{\Omega}_0 > 0. \end{cases} \tag{6.1}$$

Lemma 6.2. *The solution of problem* (6.1) *that has a perturbation function* $\Psi(\mu)$ *is provided by the following:*

$$\widehat{\Omega}(\mu) = \widehat{\Omega}_0 + \frac{\Lambda(1-\kappa)\mu^{\Lambda-1}(g(\mu, \widehat{\Omega}(\mu)) + \Psi(\mu))}{M(\kappa)} + \frac{\kappa\Lambda}{M(\kappa)} \int_0^{\mu} y^{\kappa-1}(g(y, \widehat{\Omega}(y)) + \Psi(y))dy, \quad \mu \in \mathbb{I}. \tag{6.2}$$

Proof. The proof can be obtained using Lemma 5.1. □

Theorem 6.3. *Under assumption* (A_1) *and the condition* $\frac{L_g}{M(\kappa)}\left(\Lambda\left(1-\kappa\right)T^{\Lambda-1}+\kappa T^{\Lambda}\right)<1$, *model* (5.2) *is H-U stable.*

Proof. Let $\Omega,\widehat{\Omega}\in\mathfrak{B}$ be unique and any solution of models (5.2) and (6.1), respectively. For $\mu\in(\mu_1,T]$, using (5.5) and (6.2), we have the following:

$$\begin{aligned}
&\left|\widehat{\Omega}(\mu)-\Omega(\mu)\right|\leq\frac{\Lambda(1-\kappa)\mu^{\Lambda-1}}{M(\kappa)}\left|g(\mu,\widehat{\Omega}(\mu))-g(\mu,\Omega(\mu))\right|+\frac{\kappa\Lambda}{M(\kappa)}\int_0^{\mu}y^{\kappa-1}\left|g(\mu,\widehat{\Omega}(\mu))-g(\mu,\Omega(\mu))\right|dy\\
&+\frac{\Lambda(1-\kappa)\mu^{\Lambda-1}}{M(\kappa)}\left|\Psi(\mu)\right|+\frac{\kappa\Lambda}{M(\kappa)}\int_0^{\mu}y^{\kappa-1}\left|\Psi(\mu)\right|dy\\
&\leq\frac{L_g}{M(\kappa)}\left(\Lambda\left(1-\kappa\right)T^{\Lambda-1}+\kappa T^{\Lambda}\right)\left\|\widehat{\Omega}-\Omega\right\|+\left(\frac{\Lambda(1-\kappa)T^{\Lambda-1}}{M(\kappa)}+\frac{\Lambda}{M(\kappa)}T^{\kappa}\right)\epsilon.
\end{aligned}\tag{6.3}$$

A further simplification implies the following:

$$\left\|\widehat{\Omega}-\Omega\right\|\leq\frac{\left(\frac{\Lambda(1-\kappa)T^{\Lambda-1}}{M(\kappa)}+\frac{\Lambda}{M(\kappa)}T^{\kappa}\right)}{1-\left(\frac{L_g}{M(\kappa)}\left(\Lambda\left(1-\kappa\right)T^{\Lambda-1}+\kappa T^{\Lambda}\right)\right)}\epsilon.\tag{6.4}$$

This implies that

$$\left\|\widehat{\Omega}-\Omega\right\|\leq\mathbf{c}\epsilon,$$

where

$$\mathbf{c}=\frac{\left(\frac{\Lambda(1-\kappa)T^{\Lambda-1}}{M(\kappa)}+\frac{\Lambda}{M(\kappa)}T^{\kappa}\right)}{1-\left(\frac{L_g}{M(\kappa)}\left(\Lambda\left(1-\kappa\right)T^{\Lambda-1}+\kappa T^{\Lambda}\right)\right)}.\tag{6.5}$$

This proves that model (5.2) is H-U stable. □

7. Numerical solution of (2.1)

In this section, we aim to find a numerical solution for model (5.2) under FFCFDs. To develop the numerical scheme for the proposed model, we use the extended Adams-Bashforth method (ABM) with piecewise Lagrange interpolation as used in [38]. To proceed, we first write the model in the following form:

$$\begin{cases}
{}^{CF}D_{\mu}^{\kappa}S(\mu)=\Lambda\mu^{\Lambda-1}\Omega_1(\mu,S,V,I,R,B),\\
{}^{CF}D_{\mu}^{\kappa}V(\mu)=\Lambda\mu^{\Lambda-1}\Omega_2(\mu,S,V,I,R,B),\\
{}^{CF}D_{\mu}^{\kappa}I(\mu)=\Lambda\mu^{\Lambda-1}\Omega_3(\mu,S,V,I,R,B),\\
{}^{CF}D_{\mu}^{\kappa}R(\mu)=\Lambda\mu^{\Lambda-1}\Omega_4(\mu,S,V,I,R,B),\\
{}^{CF}D_{\mu}^{\kappa}B(\mu)=\Lambda\mu^{\Lambda-1}\Omega_5(\mu,S,V,I,R,B).
\end{cases}\tag{7.1}$$

Applying the Caputo Fabrizio fractional integral to the system of Eq (7.1), we get the following:

$$\begin{cases} S = S(0) + \dfrac{\Lambda(1-\kappa)\mu^{\Lambda-1}\Omega_1(\mu,S,V,I,R,B)}{M(\kappa)} + \dfrac{\kappa\Lambda}{M(\kappa)}\displaystyle\int_0^{\mu} y^{\kappa-1}\Omega_1(y,S,V,I,R,B)dy, \\ V = V(0) + \dfrac{\Lambda(1-\kappa)\mu^{\Lambda-1}\Omega_3(\mu,S,V,I,R,B)}{M(\kappa)} + \dfrac{\kappa\Lambda}{M(\kappa)}\displaystyle\int_0^{\mu} y^{\kappa-1}\Omega_3(y,S,V,I,R,B)dy, \\ I = I(0) + \dfrac{\Lambda(1-\kappa)\mu^{\Lambda-1}\Omega_4(\mu,S,V,I,R,B)}{M(\kappa)} + \dfrac{\kappa\Lambda}{M(\kappa)}\displaystyle\int_0^{\mu} y^{\kappa-1}\Omega_4(y,S,V,I,R,B)dy, \\ R = R(0) + \dfrac{\Lambda(1-\kappa)\mu^{\Lambda-1}\Omega_5(\mu,S,V,I,R,B)}{M(\kappa)} + \dfrac{\kappa\Lambda}{M(\kappa)}\displaystyle\int_0^{\mu} y^{\kappa-1}\Omega_5(y,S,V,I,R,B)dy, \\ B = B(0) + \dfrac{\Lambda(1-\kappa)\mu^{\Lambda-1}\Omega_2(\mu,S,V,I,R,B)}{M(\kappa)} + \dfrac{\kappa\Lambda}{M(\kappa)}\displaystyle\int_0^{\mu} y^{\kappa-1}\Omega_2(y,S,V,I,R,B)dy. \end{cases} \tag{7.2}$$

At $\mu = \mu_{a+1}$, the scheme is given by the following:

$$\begin{cases} S^{a+1} = S(0) + \dfrac{\Lambda(1-\kappa)\mu_a^{\Lambda-1}\Omega_1(\mu_a,S,V,I,R,B)}{M(\kappa)} + \dfrac{\kappa\Lambda}{M(\kappa)}\displaystyle\int_0^{\mu_a} y^{\kappa-1}\Omega_1(y,S,V,I,R,B)dy, \quad \mu_a \in \mathbb{I}, \\ V^{a+1} = V(0) + \dfrac{\Lambda(1-\kappa)\mu_a^{\Lambda-1}\Omega_3(\mu_a,S,V,I,R,B)}{M(\kappa)} + \dfrac{\kappa\Lambda}{M(\kappa)}\displaystyle\int_0^{\mu_a} y^{\kappa-1}\Omega_3(y,S,V,I,R,B)dy, \quad \mu_a \in \mathbb{I}, \\ I^{a+1} = I(0) + \dfrac{\Lambda(1-\kappa)\mu_a^{\Lambda-1}\Omega_4(\mu_a,S,V,I,R,B)}{M(\kappa)} + \dfrac{\kappa\Lambda}{M(\kappa)}\displaystyle\int_0^{\mu_a} y^{\kappa-1}\Omega_4(y,S,V,I,R,B)dy, \quad \mu_a \in \mathbb{I}, \\ R^{a+1} = R(0) + \dfrac{\Lambda(1-\kappa)\mu_a^{\Lambda-1}\Omega_5(\mu_a,S,V,I,R,B)}{M(\kappa)} + \dfrac{\kappa\Lambda}{M(\kappa)}\displaystyle\int_0^{\mu_a} y^{\kappa-1}\Omega_5(y,S,V,I,R,B)dy, \quad \mu_a \in \mathbb{I}, \\ B^{a+1} = B(0) + \dfrac{\Lambda(1-\kappa)\mu_a^{\Lambda-1}\Omega_2(\mu_a,S,V,I,R,B)}{M(\kappa)} + \dfrac{\kappa\Lambda}{M(\kappa)}\displaystyle\int_0^{\mu_a} y^{\kappa-1}\Omega_2(y,S,V,I,R,B)dy, \quad \mu_a \in \mathbb{I}. \end{cases} \tag{7.3}$$

Now, take the difference between the consecutive terms to obtain the following:

$$\begin{cases} S^{a+1} = \begin{cases} S(0) + \frac{\Lambda(1-\kappa)\mu_a^{\Lambda-1}\Omega_1(\mu_a,S^a,V^a,I^a,R^a,B^a)}{M(\kappa)} - \frac{\Lambda(1-\kappa)\mu_{a-1}^{\Lambda-1}\Omega_1(\mu_{a-1},S^{a-1},V^{a-1},I^{a-1},R^{a-1},B^{a-1})}{M(\kappa)} \\ \quad + \frac{\kappa\Lambda}{M(\kappa)}\int_{\mu_a}^{\mu_{a+1}} y^{\kappa-1}\Omega_1(y,S,V,I,R,B)dy, \quad \mu_a,\mu_{a+1} \in \mathbb{I}, \end{cases} \\ V^{a+1} = \begin{cases} V(0) + \frac{\Lambda(1-\kappa)\mu_a^{\Lambda-1}\Omega_3(\mu_a,S^a,V^a,I^a,R^a,B^a)}{M(\kappa)} - \frac{\Lambda(1-\kappa)\mu_{a-1}^{\Lambda-1}\Omega_3(\mu_{a-1},S^{a-1},V^{a-1},I^{a-1},R^{a-1},B^{a-1})}{M(\kappa)} \\ \quad + \frac{\kappa\Lambda}{M(\kappa)}\int_{\mu_a}^{\mu_{a+1}} y^{\kappa-1}\Omega_3(y,S,V,I,R,B)dy, \quad \mu_a,\mu_{a+1} \in \mathbb{I}, \end{cases} \\ I^{a+1} = \begin{cases} I(0) + \frac{\Lambda(1-\kappa)\mu_a^{\Lambda-1}\Omega_4(\mu_a,S^a,V^a,I^a,R^a,B^a)}{M(\kappa)} - \frac{\Lambda(1-\kappa)\mu_{a-1}^{\Lambda-1}\Omega_4(\mu_{a-1},S^{a-1},V^{a-1},I^{a-1},R^{a-1},B^{a-1})}{M(\kappa)} \\ \quad + \frac{\kappa\Lambda}{M(\kappa)}\int_{\mu_a}^{\mu_{a+1}} y^{\kappa-1}\Omega_4(y,S,V,I,R,B)dy, \quad \mu_a,\mu_{a+1} \in \mathbb{I}, \end{cases} \\ R^{a+1} = \begin{cases} R(0) + \frac{\Lambda(1-\kappa)\mu_a^{\Lambda-1}\Omega_5(\mu_a,S^a,V^a,I^a,R^a,B^a)}{M(\kappa)} - \frac{\Lambda(1-\kappa)\mu_{a-1}^{\Lambda-1}\Omega_5(\mu_{a-1},S^{a-1},V^{a-1},I^{a-1},R^{a-1},B^{a-1})}{M(\kappa)} \\ \quad + \frac{\kappa\Lambda}{M(\kappa)}\int_{\mu_a}^{\mu_{a+1}} y^{\kappa-1}\Omega_5(y,S,V,I,R,B)dy, \quad \mu_a,\mu_{a+1} \in \mathbb{I}. \end{cases} \\ B^{a+1} = \begin{cases} B(0) + \frac{\Lambda(1-\kappa)\mu_a^{\Lambda-1}\Omega_2(\mu_a,S^a,V^a,I^a,R^a,B^a)}{M(\kappa)} - \frac{\Lambda(1-\kappa)\mu_{a-1}^{\Lambda-1}\Omega_2(\mu_{a-1},S^{a-1},V^{a-1},I^{a-1},R^{a-1},B^{a-1})}{M(\kappa)} \\ \quad + \frac{\kappa\Lambda}{M(\kappa)}\int_{\mu_a}^{\mu_{a+1}} y^{\kappa-1}\Omega_2(y,S,V,I,R,B)dy, \quad \mu_a,\mu_{a+1} \in \mathbb{I}. \end{cases} \end{cases} \tag{7.4}$$

Integrating, and employing a Lagrangian interpolation to approximate the kernels leads to the following:

$$\begin{cases} S^{a+1} = \begin{cases} S(0) + \frac{\Lambda(1-\kappa)\mu_a^{\Lambda-1}\Omega_1(\mu_a,S^a,V^a,I^a,R^a,B^a)}{M(\kappa)} - \frac{\Lambda(1-\kappa)\mu_{a-1}^{\Lambda-1}\Omega_1(\mu_{a-1},S^{a-1},V^{a-1},I^{a-1},R^{a-1},B^{a-1})}{M(\kappa)} \\ +\frac{\Lambda\kappa}{M(\kappa)}\frac{3}{2}(\Delta\mu)\mu_a^{\Lambda-1}\Omega_1(\mu_a,S^a,V^a,I^a,R^a,B^a) - \frac{\Lambda\kappa}{M(\kappa)}\frac{(\Delta\mu)}{2}\mu_{a-1}^{\Lambda-1}\Omega_1(\mu_{a-1},S^{a-1},V^{a-1},I^{a-1},R^{a-1},B^{a-1}), \\ \mu_a,\mu_{a-1}\in\mathbb{I}, \end{cases} \\ V^{a+1} = \begin{cases} V(0) + \frac{\Lambda(1-\kappa)\mu_a^{\Lambda-1}\Omega_3(\mu_a,S^a,V^a,I^a,R^a,B^a)}{M(\kappa)} - \frac{\Lambda(1-\kappa)\mu_{a-1}^{\Lambda-1}\Omega_3(\mu_{a-1},S^{a-1},V^{a-1},I^{a-1},R^{a-1},B^{a-1})}{M(\kappa)} \\ +\frac{\Lambda\kappa}{M(\kappa)}\frac{3}{2}(\Delta\mu)\mu_a^{\Lambda-1}\Omega_3(\mu_a,S^a,V^a,I^a,R^a,B^a) - \frac{\Lambda\kappa}{M(\kappa)}\frac{(\Delta\mu)}{2}\mu_{a-1}^{\Lambda-1}\Omega_3(\mu_{a-1},S^{a-1},V^{a-1},I^{a-1},R^{a-1},B^{a-1}), \\ \mu_a,\mu_{a-1}\in\mathbb{I}, \end{cases} \\ I^{a+1} = \begin{cases} I(0) + \frac{\Lambda(1-\kappa)\mu_a^{\Lambda-1}\Omega_4(\mu_a,S^a,V^a,I^a,R^a,B^a)}{M(\kappa)} - \frac{\Lambda(1-\kappa)\mu_{a-1}^{\Lambda-1}\Omega_4(\mu_{a-1},S^{a-1},V^{a-1},I^{a-1},R^{a-1},B^{a-1})}{M(\kappa)} \\ +\frac{\Lambda\kappa}{M(\kappa)}\frac{3}{2}(\Delta\mu)\mu_a^{\Lambda-1}\Omega_4(\mu_a,S^a,V^a,I^a,R^a,B^a) - \frac{\Lambda\kappa}{M(\kappa)}\frac{(\Delta\mu)}{2}\mu_{a-1}^{\Lambda-1}\Omega_4(\mu_{a-1},S^{a-1},V^{a-1},I^{a-1},R^{a-1},B^{a-1}), \\ \mu_a,\mu_{a-1}\in\mathbb{I}, \end{cases} \\ R^{a+1} = \begin{cases} R(0) + \frac{\Lambda(1-\kappa)\mu_a^{\Lambda-1}\Omega_5(\mu_a,S^a,V^a,I^a,R^a,B^a)}{M(\kappa)} - \frac{\Lambda(1-\kappa)\mu_{a-1}^{\Lambda-1}\Omega_5(\mu_{a-1},S^{a-1},V^{a-1},I^{a-1},R^{a-1},B^{a-1})}{M(\kappa)} \\ +\frac{\Lambda\kappa}{M(\kappa)}\frac{3}{2}(\Delta\mu)\mu_a^{\Lambda-1}\Omega_5(\mu_a,S^a,V^a,I^a,R^a,B^a) - \frac{\Lambda\kappa}{M(\kappa)}\frac{(\Delta\mu)}{2}\mu_{a-1}^{\Lambda-1}\Omega_5(\mu_{a-1},S^{a-1},V^{a-1},I^{a-1},R^{a-1},B^{a-1}), \\ \mu_a,\mu_{a-1}\in\mathbb{I}. \end{cases} \\ B^{a+1} = \begin{cases} B(0) + \frac{\Lambda(1-\kappa)\mu_a^{\Lambda-1}\Omega_2(\mu_a,S^a,V^a,I^a,R^a,B^a)}{M(\kappa)} - \frac{\Lambda(1-\kappa)\mu_{a-1}^{\Lambda-1}\Omega_2(\mu_{a-1},S^{a-1},V^{a-1},I^{a-1},R^{a-1},B^{a-1})}{M(\kappa)} \\ +\frac{\Lambda\kappa}{M(\kappa)}\frac{3}{2}(\Delta\mu)\mu_a^{\Lambda-1}\Omega_2(\mu_a,S^a,V^a,I^a,R^a,B^a) - \frac{\Lambda\kappa}{M(\kappa)}\frac{(\Delta\mu)}{2}\mu_{a-1}^{\Lambda-1}\Omega_2(\mu_{a-1},S^{a-1},V^{a-1},I^{a-1},R^{a-1},B^{a-1}), \\ \mu_a,\mu_{a-1}\in\mathbb{I}. \end{cases} \end{cases} \tag{7.5}$$

This iteration scheme gives the numerical solution of the proposed mathematical model.

8. Simulations and discussion

In this section, using the parameters values in Table 1 and the initial conditions S(0)=850, V(0)=50, I(0)=50, R(0)=40, and B(0)=10, we simulate the numerical results under fractional-order and fractal-dimensional variations to observe the dynamics of different compartments of the proposed SVIRB model. The simulations were performed using MATLAB R2023a.

To confirm the reliability of the proposed numerical method, we compare it with the Runge-Kutta 4th Order (RK-4) numerical method.

In Figure 3, we observe that the results of our simulations reveal a strong agreement between the numerical solutions obtained using the ABM method and the classical RK-4 approach under integer-order derivatives. Hence, the ABM method is well behaved. Previous investigations such as [39] have similarly demonstrated the accuracy of the ABM method to solve the initial value problems, thus supporting its application in the current context. Then, we proceeded to examine the effects of varying the fractional order and fractal dimension independently. These parameters serve to represent key epidemiological features in the model: The fractional order is associated with the memory or history-dependence of disease transmission and immunity, while the fractal dimension characterizes structural heterogeneity within the population, such as differences in social contact patterns, access to healthcare,

or vaccine coverage.

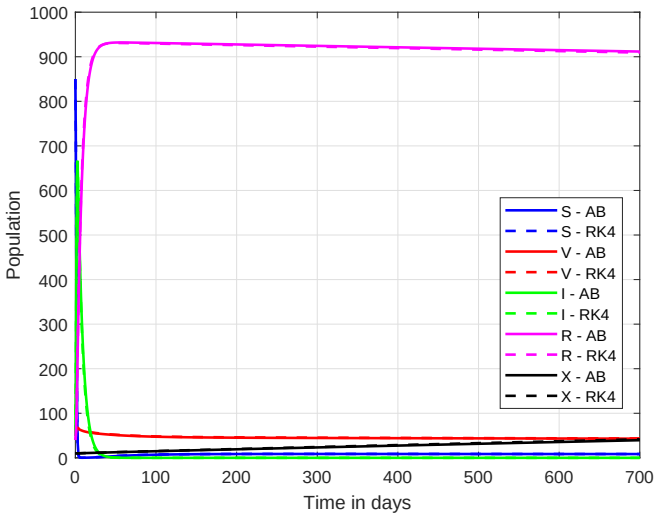

Figure 3. Solution plots of rotavirus-SVIRB model by RK-4 and ABM numerical methods.

In Figure 4, we investigate how changes in the fractional order influence the disease dynamics while keeping the fractal dimension fixed. This allows us to isolate the impact of memory effects. The evolution of the susceptible population (sub-figure 4a) shows a decrease as individuals either receive vaccinations or become infected. Higher values of the fractional order lead to a more rapid stabilization of this class, which indicates a quicker transition of individuals due to weaker memory effects. This behavior aligns with real-life scenarios, where immunity develops swiftly and past exposure has a limited impact on the present dynamics. Conversely, lower fractional orders reflect stronger memory effects, which is consistent with populations where immunity either builds up or wanes more gradually. The dynamics of the vaccinated group (sub-figure 4b) exhibit an initial increase, followed by a decline as individuals either transition to the booster class or become infected. As the fractional order increases, this transition occurs more rapidly, thus demonstrating the sensitivity of vaccination dynamics to memory effects. The infected class (sub-figure 4c) shows a moderate peak and subsequent decline, which reflects effective disease control through vaccination. Higher fractional orders are associated with quicker containment, which could represent efficient immunization campaigns. Similarly, the recovered class (sub-figure 4d) steadily rises, and its growth rate improves with an increasing fractional order, thus highlighting more effective recovery dynamics. In sub-figure 4e, the booster-immunized population increases due to transitions from the vaccinated class. However, the growth rate slows down over time due to reinfection risks, which are particularly governed by the booster infection factor. These dynamics suggest that the fractional order can model immune memory and the timing of immunity waning or reactivation. Figure 5 focuses on the impact of varying the fractal dimension while keeping the fractional order constant. This isolates the effect of population heterogeneity and spatial complexity on the disease spread. The results show that different values of the fractal dimension lead to distinct dynamics in all compartments, even with identical vaccination strategies. This suggests that local differences in contact patterns, healthcare accessibility, and booster coverage can significantly influence the disease outcomes. Such findings reflect real-world observations where rural and urban populations respond differently to the same immunization policy due to structural disparities. The

results underscore the importance of incorporating booster vaccination strategies and region-specific planning in public health programs. Additionally, they highlight the limitations of conventional models that ignore these complexities. By using a fractal-fractional approach, our model offers a more nuanced view of disease evolution and can serve as a useful tool to design and optimize vaccination interventions.

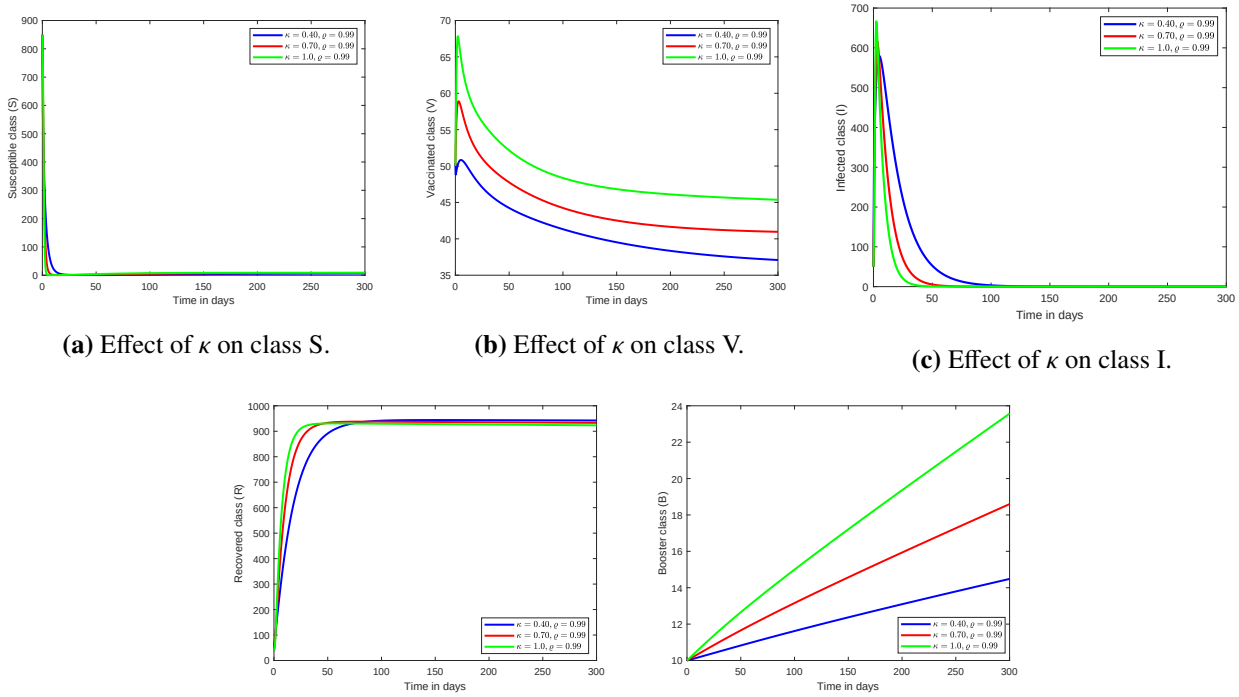

(a) Effect of κ on class S. **(b)** Effect of κ on class V. **(c)** Effect of κ on class I.

(d) Effect of κ on class R. **(e)** Effect of κ on class B.

Figure 4. Impact of fractional order derivative on the dynamical behavior of rotavirus-SVIRB model.

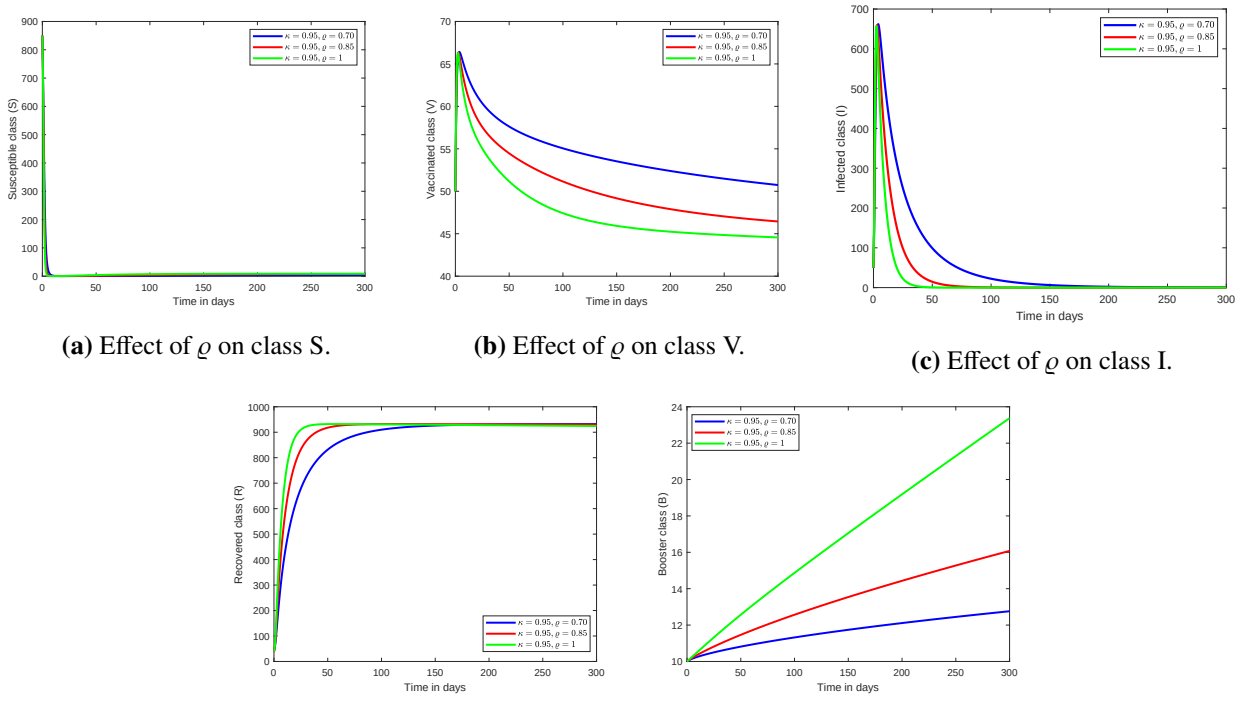

(a) Effect of ϱ on class S. **(b)** Effect of ϱ on class V. **(c)** Effect of ϱ on class I.

(d) Effect of ϱ on class R. **(e)** Effect of ϱ on class B.

Figure 5. Impact of fractal dimension on the dynamical behavior of rotavirus-SVIRB model.

9. Conclusions

In this work, we developed and analyzed a fractal-fractional mathematical model for rotavirus transmission that incorporates both primary and booster vaccination strategies. By employing the Caputo-Fabrizio derivative, the model successfully captured the memory-dependent and non-local nature of disease dynamics. The analysis of equilibrium points, supported by the computation of the basic reproduction number, provided critical insights into the conditions under which the disease can be eradicated or persist.

The simulation results demonstrate that variations in the fractional order and fractal dimension notably affect the timing, peak intensity, and transient dynamics of rotavirus spread. Although the overall number of infections remains comparable, these subtle yet impactful differences can be critical from a public health standpoint. Specifically, shifts in the outbreak timing can be influential when healthcare systems experience a peak load, and when preventive measures such as vaccination campaigns, awareness drives, or lockdowns should be implemented. The inclusion of fractional derivatives introduces memory effects, thereby accounting for the influence of past states on the present dynamics, which is a feature absent in classical models.

In the present study, the model parameters were selected to observe the qualitative behavior of the system under various fractal-fractional orders. No data fitting was performed. As a direction for future work, the model can be calibrated against real epidemiological data using parameter estimation techniques. This would allow for an improved accuracy in forecasting an disease dynamics, evaluating intervention strategies (e.g., booster dose effectiveness), and enhancing the model's applicability to

real-world public health planning.

Author contributions

A. Ali: Writing – original draft; A. A. Qurtam: Funding acquisition; R. Sidaoui: Conceptualization, methodology, and writing – review and editing; M. Suhail: Supervision, project administration; K. Aldwoah: Formal analysis, validation; A. Elsayed: Visualization, writing – review and editing; E. I. Hassan: Writing – review and editing. All authors have read and agreed to the published version of the manuscript.

Use of Generative-AI tools declaration

The authors declare that they have not used Artificial Intelligence (AI) tools in the creation of this article.

Acknowledgments

This work was supported and funded by the Deanship of Scientific Research at Imam Mohammad Ibn Saud Islamic University (IMSIU) (grant number IMSIU-DDRSP2501).

Conflict of interest

The authors declare that they have no conflicts of interest.

References

1. L. J. White, J. Buttery, B. Cooper, D. J. Nokes, G. Medley, Rotavirus within day care centres in Oxfordshire, UK: Characterization of partial immunity, *J. R. Soc. Interface*, **5** (2008), 1481–1490. https://doi.org/10.1098/rsif.2008.0115
2. WHO: World Health Organization, *Generic protocol for monitoring impact of rotavirus vaccination on gastroenteritis disease burden and viral strains*, Geneva, 2008. Available from: http://www.emro.who.int/health-topics/rotavirus-gastroenteritis/.
3. E. Shim, H. Banks, C. Castillo-Chavez, Seasonality of rotavirus infection with its vaccination, *Contemp. Math.*, **410** (2006), 327–347. https://doi.org/10.1090/conm/410/07735
4. E. J. Anderson, S. G. Weber, Rotavirus infection in adults, *Lancet Infect. Dis.*, **4** (2004), 91–99. https://doi.org/10.1016/S1473-3099(04)00928-4
5. T. Ruuska, T. Vesikari, Rotavirus disease in Finnish children: Use of numerical scores for clinical severity of diarrhoeal episodes, *Scand. J. Infect. Dis.*, **22** (1990), 259–267. https://doi.org/10.3109/00365549009027046
6. R. F. Bishop, Natural history of human rotavirus infection, *Arch. Virol.*, **12** (1996), 119–128. Available from: https://link.springer.com/chapter/10.1007/978-3-7091-6553-9_14.

7. P. H. Dennehy, Transmission of rotavirus and other enteric pathogens in the home, *Pediatr. Infect. Dis. J.*, **19** (2000), S103–S105. https://doi.org/10.1097/00006454-200010001-00003
8. L. W. Nitiema, J. Nordgren, D. Ouermi, D. Dianou, A. S. Traore, L. Svensson, et al., Burden of rotavirus and other enteropathogens among children with diarrhea in Burkina Faso, *Int. J. Infect. Dis.*, **15** (2011), 646–652. https://doi.org/10.1016/j.ijid.2011.05.009
9. T. Snelling, P. Markey, J. Carapetis, R. Andrews, Rotavirus infection in Northern Territory before and after vaccination, *Microbiol. Aust.*, **33** (2012), 61–63. https://doi.org/10.1071/MA12061
10. Y. Wang, Z. Jin, Z. Yang, Z. K. Zhang, T. Zhou, G. Q. Sun, Global analysis of an SIS model with an infective vector on complex networks, *Nonlinear Anal.-Real*, **13** (2012), 543–557. https://doi.org/10.1016/j.nonrwa.2011.07.033
11. Y. Wang, Z. Jin, Global analysis of multiple routes of disease transmission on heterogeneous networks, *Physica A*, **392** (2013), 3869–3880. https://doi.org/10.1016/j.physa.2013.03.042
12. C. E. Okafor, Introducing rotavirus vaccination in Nigeria: Economic evaluation and implications, *Pharmacoecon.-Open*, **5** (2021), 545–557. https://doi.org/10.1007/s41669-020-00251-6
13. P. Jain, A. Jain, *Waterborne viral gastroenteritis: An introduction to common agents*, Water and Health, Springer, Berlin, 2014, 53–74. https://doi.org/10.1007/978-81-322-1029-0_4
14. U. D. Parashar, E. G. Hummelman, J. S. Bresee, M. A. Miller, R. I. Glass, Global illness and deaths caused by rotavirus disease in children, *Emerg. Infect. Dis.*, **9** (2003), 565–572. https://doi.org/10.3201/eid0905.020562
15. E. K. Yeargers, R. W. Shonkwiler, J. V. Herod, *An introduction to the mathematics of biology: With computer algebra models*, Springer, 2013.
16. K. A. Aldwoah, M. A. Almalahi, M. Hleili, F. A. Alqarni, E. S. Aly, K. Shah, Analytical study of a modified-ABC fractional order breast cancer model, *J. Appl. Math. Comput.*, **70** (2024), 3685–3716. https://doi.org/10.1007/s12190-024-02102-7
17. H. Khan, J. Alzabut, A. Shah, Z. Y. He, S. Etemad, S. Rezapour, et al., On fractal-fractional waterborne disease model: A study on theoretical and numerical aspects of solutions via simulations, *Fractals*, **31** (2023), 2340055. https://doi.org/10.1142/S0218348X23400558
18. S. E. Shuaib, P. Riyapan, A mathematical model to study the effects of breastfeeding and vaccination on rotavirus epidemics, *J. Math. Fundam. Sci.*, **52** (2020), 43–65. https://doi.org/10.5614/j.math.fund.sci.2020.52.1.4
19. N. B. Ilmi, I. Darti, A. Suryanto, Dynamical analysis of a rotavirus infection model with vaccination and saturation incidence rate, *J. Phys.: Conf. Ser.*, **1562** (2020), 012018. https://doi.org/10.1088/1742-6596/1562/1/012018
20. F. Weidemann, M. Dehnert, J. Koch, O. Wichmann, M. Höhle, Bayesian parameter inference for dynamic infectious disease modelling: Rotavirus in Germany, *Stat. Med.*, **33** (2014), 1580–1599. https://doi.org/10.1002/sim.6041
21. A. Atangana, Fractal-fractional differentiation and integration: Connecting fractal calculus and fractional calculus to predict complex system, *Chaos Soliton. Fract.*, **102** (2017), 396–406. https://doi.org/10.1016/j.chaos.2017.04.027

22. A. E. Hamza, O. Osman, A. Ali, A. Alsulami, K. Aldwoah, A. Mustafa, et al., Fractal-fractional-order modeling of liver fibrosis disease and its mathematical results with subinterval transitions, *Fractal Fract.*, **8** (2024), 638. https://doi.org/10.3390/fractalfract8110638

23. T. A. Burton, A fixed-point theorem of Krasnoselskii, *Appl. Math. Lett.*, **11** (1998), 85–88. https://doi.org/10.1016/S0893-9659(97)00138-9

24. J. Peinadoa, J. Ibáñeza, E. Ariasb, V. Hernández, Adams-Bashforth and Adams-Moulton methods for solving differential Riccati equations, *Comput. Math. Appl.*, **60** (2010), 3032–3045. https://doi.org/10.1016/j.camwa.2010.10.002

25. R. Singh, J. Mishra, V. K. Gupta, Dynamical analysis of a tumor growth model under the effect of fractal fractional Caputo-Fabrizio derivative, *Int. J. Math. Comput. Eng.*, **1** (2023), 115–126. https://doi.org/10.2478/ijmce-2023-0009

26. W. Al-Sadi, Z. Wei, I. Moroz, A. Alkhazzan, Existence and stability of solution in Banach space for an impulsive system involving Atangana-Baleanu and Caputo-Fabrizio derivatives, *Fractals*, **31** (2023), 2340085. https://doi.org/10.1142/S0218348X23400856

27. Y. Tian, F. Yu, G. Zhang, C. Tian, X. Wang, Y. Chen, et al., Rotavirus outbreaks in China, 1982-2021: A systematic review, *Front. Public Health*, **12** (2024), 1423573. https://doi.org/10.3389/fpubh.2024.1423573

28. W. Al-Sadi, Z. Wei, T. Q. Abdullah, A. Alkhazzan, J. F. Gómez-Aguilar, Dynamical and numerical analysis of the hepatitis B virus treatment model through fractal-fractional derivative, *Math. Method. Appl. Sci.*, **48** (2025), 639–657. https://doi.org/10.1002/mma.10348

29. O. L. Omondi, C. Wang, X. Xue, O. G. Lawi, Modeling the effects of vaccination on rotavirus infection, *Adv. Differ. Equ.*, **2015** (2015), 381. https://doi.org/10.1186/s13662-015-0722-1

30. K. Eiman, K. Shah, M. Sarwar, T. Abdeljawad, On rotavirus infectious disease model using piecewise modified ABC fractional order derivative, *Netw. Heterog. Media*, **19** (2024), 1. https://doi.org/10.3934/nhm.2024010

31. N. M. Laban, S. Bosomprah, M. Simuyandi, M. Chibuye, A. Chauwa, M. Chirwa-Chobe, et al., Evaluation of ROTARIX booster dose vaccination at 9 months for safety and enhanced anti-rotavirus immunity in Zambian children: A randomised controlled trial, *Vaccines*, **11** (2023), 346. https://doi.org/10.3390/vaccines11020346

32. E. Burnett, B. A. Lopman, U. D. Parashar, Potential for a booster dose of rotavirus vaccine to further reduce diarrhea mortality, *Vaccine*, **35** (2017), 7198–7203. https://doi.org/10.1016/j.vaccine.2017.10.027

33. F. C. Haidara, M. D. Tapia, S. O. Sow, M. Doumbia, F. Coulibaly, F. Diallo, et al., Evaluation of a booster dose of pentavalent rotavirus vaccine coadministered with measles, yellow fever, and meningitis A vaccines in 9-month-old Malian infants, *J. Infect. Dis.*, **218** (2018), 606–613. https://doi.org/10.1093/infdis/jiy215

34. S. Ahmad, A. Ullah, M. Arfan, K. Shah, On analysis of the fractional mathematical model of rotavirus epidemic with the effects of breastfeeding and vaccination under Atangana-Baleanu (AB) derivative, *Chaos Soliton. Fract.*, **140** (2020), 110233. https://doi.org/10.1016/j.chaos.2020.110233

35. R. F. Bishop, G. Davidson, I. Holmes, B. Ruck, Virus particles in epithelial cells of duodenal mucosa from children with acute non-bacterial gastroenteritis, *Lancet*, **302** (1973), 1281–1283. https://doi.org/10.1016/S0140-6736(73)92867-5

36. A. Eigenwillig, *Real root isolation for exact and approximate polynomials using Descartes' rule of signs*, PhD thesis, Saarland University, 2008.

37. I. A. Rus, Ulam stabilities of ordinary differential equations in a Banach space, *Carpath. J. Math.*, **26** (2010), 103–107.

38. M. A. Khan, A. Atangana, *Numerical methods for fractal-fractional differential equations and engineering simulations and modeling*, CRC Press, 2023. https://doi.org/10.1201/9781003359258

39. Marsudi, I. Darti, A comparative study on numerical solutions of initial values problems of differential equations using the three numerical methods, *BAREKENG J. Math. Appl.*, **19** (2025), 1263–1278. https://doi.org/10.30598/barekengvol19iss2pp1263-1278

AIMS Press